JCI The Journal of Clinical Investigation

CD73 Immune Checkpoint Defines Regulatory NK-cells within the Tumor Microenvironment

Shi Yong Neo, … , Johan Hartman, Andreas Lundqvist

J Clin Invest. 2019. https://doi.org/10.1172/JCI128895.

Research In-Press Preview Immunology

Graphical abstract

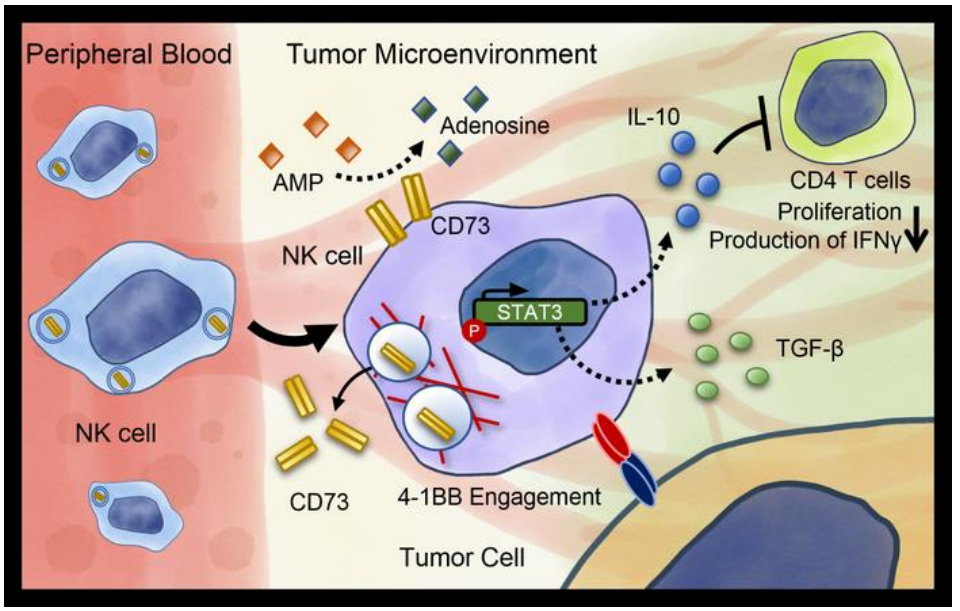

CD73 Immune Checkpoint Defines Regulatory NK-cells within the Tumor Microenvironment

Neo Shi Yong[1], Yang Ying[1,2], Record Julien[3], Ma Ran[1], Chen Xinsong[1], Chen Ziqing[1], Tobin Nicholas P[1], Blake Emily[4], Seitz Christina[5], Thomas Ron[4], Wagner Arnika Kathleen[6], Andersson John[5], de Boniface Jana[7,8], Bergh Jonas[1], Murray Shannon[9], Alici Evren[6], Childs Richard[10], Johansson Martin[11], Westerberg Lisa S[4], Haglund Felix[1], Hartman Johan[1,12], Lundqvist Andreas[1]

[1] Department of Oncology-Pathology, Karolinska Institutet, Stockholm, Sweden.
[2] Department of Respiratory Medicine, Second Affiliated Hospital, Zhejiang University School of Medicine, Hangzhou, China.
[3] Department of Microbiology, Tumor and Cell Biology, Karolinska Institutet, Stockholm, Sweden.
[4] Cell Therapy Institute, Nova Southeastern University, Fort Lauderdale, FL, USA.
[5] Department of Medical Epidemiology and Biostatistics, Karolinska Institutet, Stockholm, Sweden
[6] Department of Medicine Huddinge, Karolinska Institutet, Stockholm, Sweden
[7] Department of Molecular Medicine and Surgery, Karolinska Institutet, Stockholm, Sweden
[8] Dept. of Surgery, Capio St. Goran's Hospital, Stockholm, Sweden.
[9] Fred Hutchinson Cancer Research Center, Division of Basic Sciences, 1100 Fairview Ave. N, Seattle, USA.
[10] Laboratory of Transplantation Immunotherapy, Hematology Branch, National Heart Lung and Blood Institute, National Institutes of Health, Bethesda, MD, USA.
[11]Glactone Pharma Development AB, Helsingborg, Sweden.
[12]Department of Pathology, Karolinska University Laboratory, Södersjukhuset, Stockholm, Sweden.

Disclosures: Martin Johansson is an employee at Glactone Pharma Development.

The other authors declare no conflict of interest.

Corresponding Author:

Andreas Lundqvist

Department of Oncology-Pathology, Karolinska Institutet

Bioclinicum J6:10, Akademiska Stråket 1, Solna, Sweden 17164

Phone: +46 (0) 8-517 768 59

Email: andreas.lundqvist@ki.se

Abstract

High levels of ecto-5'-nucleotidase (CD73) have been implicated in immune suppression and tumor progression, and have also been observed in cancer patients who progress on anti-PD-1 immunotherapy. While regulatory T cells can express CD73 and inhibit T cell responses via the production of adenosine, less is known about CD73 expression in other immune cell populations. We found that tumor-infiltrating NK cells upregulate CD73 expression and the frequency of these CD73+ NK cells correlated with larger tumor size in breast cancer patients. In addition, the expression of multiple alternative immune checkpoint receptors including LAG-3, VISTA, PD-1, and PD-L1 was significantly higher in CD73 positive NK cells than in CD73 negative NK cells. Mechanistically, NK cells transport CD73 in intracellular vesicles to the cell surface and the extracellular space via actin polymerization-dependent exocytosis upon engagement of 4-1BBL on tumor cells. These CD73 positive NK cells undergo transcriptional reprogramming and upregulate IL10 production via STAT3 transcriptional activity, suppressing CD4 T cell proliferation and IFNγ production. Taken together, our results support that tumors can hijack NK cells as a means to escape immunity and that CD73 expression defines an inducible population of NK cells with immune regulatory properties within the tumor microenvironment.

58 Graphical Abstract

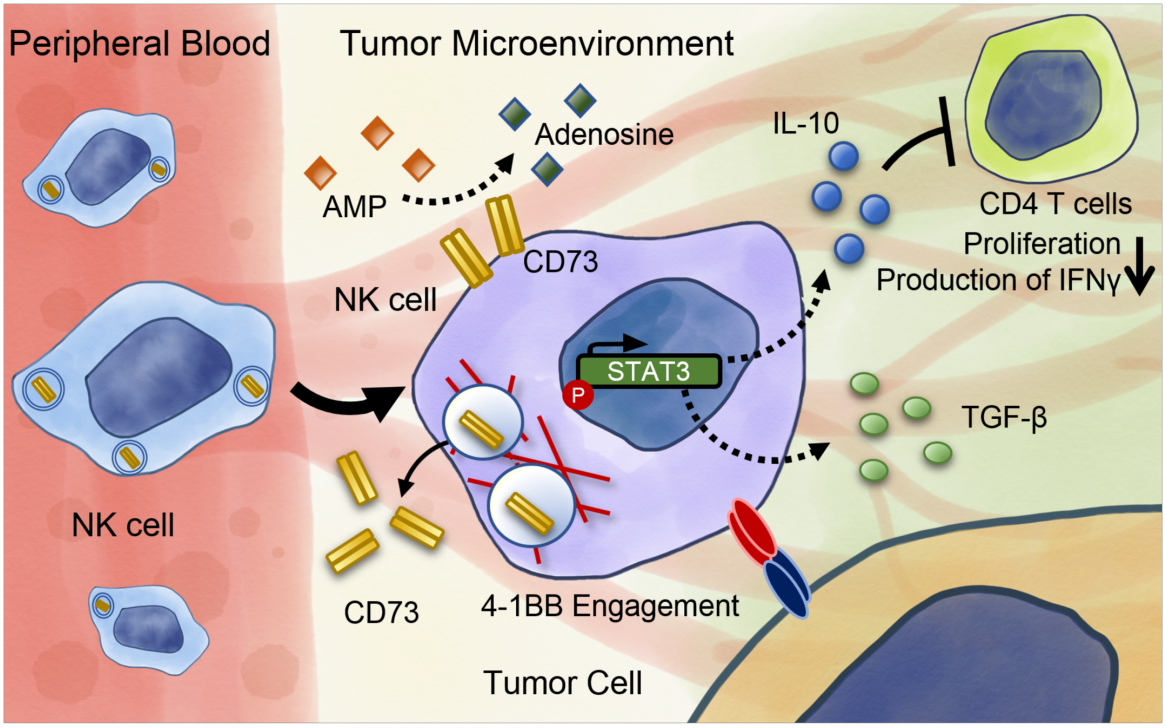

59

Introduction

The CD73 metabolic immune checkpoint orchestrates a crucial homeostatic balance of extracellular adenosine levels as part of a negative feedback mechanism to control inflammatory responses within a stressed or damaged tissue microenvironment. (1) The lack of CD73 expression could implicate physiological wound healing and immunomodulation within the tissue microenvironment. (2) Within the tumor microenvironment (TME), however, metabolic stress accumulates along with tumor progression, which leads to a dysregulated expression and activity of CD73 in cancers including breast cancer, metastatic melanoma and ovarian cancer. (3-6) Overexpression of CD73 within a tumor not only contributes to metastasis and anthracycline resistance, but also to immune evasion due to dysregulation of adenosine production. (6, 7) For these reasons, inhibitors of CD73 are today used in cancer immunotherapy in combination with existing cancer treatment including anti-PD-1/anti-PD-L1 therapy.(1, 8-11)

Tumor progression on immune checkpoint therapy can be associated with defects in tumor antigen presentation, which results in lack of tumor cell recognition by T cells. (12) This has inspired the development of therapies based on activating Natural Killer (NK) cells. (13) NK cells are characterized as granular lymphocytes capable of producing an abundance of inflammatory cytokines and induce cytotoxic responses against viral-infected and transformed cells. The regulation of their functions involves sophisticated mechanisms with a wide repertoire of signals from inhibitory and activating receptors, at the same time influenced by the type of cytokines and surrounding cells in the microenvironment. (14-16) While NK cells rarely infiltrate tumors, their presence in tumor biopsies has been shown to

positively associate with increased survival. (17) A recent clinical study investigated the clinical relevance of tumor-infiltrating NK cells in triple negative breast cancer and reported a higher overall survival probability in patients with higher frequency of tumor-infiltrating NK cells. (18) For these reasons, modulation of NK cell activity by tumor-targeting antibody therapies, immunomodulatory antibodies, cytokines, infusion of NK cells activated ex vivo, and bi-specific killer engagers are currently being explored in clinical trials. (19, 20)

Although NK cells are thought to contribute to tumor eradication, studies have established that NK cells can acquire a regulatory cell identity in acute infection and inflammation, producing adenosine and IL-10. (21, 22) More recently in the context of cancer, CD56+ CD3- cells in patients with ovarian cancer suppressed the growth of T cells as observed within an ex vivo expansion of tumor infiltrating lymphocytes (TILs). Even though it was demonstrated that the suppression was mediated by NKp46 engagement, the underlying mechanisms of how NK cells suppress are still unclear. (23) It is also still unclear how conventional NK cells can undergo a phenotypic switch to suppress other TIL populations and contribute to tumor immune escape.

We sought to investigate how peripheral blood and tumor-infiltrating NK cells differ in patients with breast cancer and sarcoma, and if tumor-infiltrating NK cells develop immune regulatory functions. Compared with peripheral blood NK cells, tumor-infiltrating NK cells undergo phenotypic changes and acquire the expression of several immune checkpoint receptors. The expression of these immune checkpoint molecules was significantly higher on NK cells expressing CD73.

Mechanistically, NK cells acquire CD73 surface expression via actin polymerization-dependent exocytosis upon engagement of 4-1BBL. These CD73+ NK cells are reprogrammed to upregulate IL10 and TGFβ production via STAT3 transcriptional activity, suppressing CD4 T cell activity. Finally, we found that the NK cell signature influenced the predictive value of CD73 gene expression in the progression-free interval of sarcoma and breast cancer. Our results demonstrate that tumor cells can influence NK cells to acquire suppressive functions independent of CD73 activity.

Results

NK cell signature influences the predictive value of CD73 gene expression in progression-free interval of sarcoma and breast cancer.

To determine the clinical relevance and relationship between NK cells and *NT5E* (encoding CD73) expression, we examined the TCGA (The Cancer Genome Atlas) database, particularly focusing on breast and sarcoma patient cohorts. As reported earlier for several other solid tumors (24), a higher *NT5E* gene expression in breast cancer correlated with worse prognosis. (Figure 1A) Using a five-gene NK cell signature that was previously applied to analyze overall survival in solid tumors including breast cancer (25), progression-free survival comparing samples stratified by the top and bottom quartiles of the NK cell signature was analyzed in relation to *NT5E* gene expression. In breast cancer, the expression of *NT5E* had a greater influence on the progression-free survival (Hazard Ratio = 2.3, 95% Confidence Interval = 1.3 - 4.1) in patients with low NK cell gene signature (Figure 1B and C) In sarcoma, however, *NT5E* expression alone do not correlate with poorer prognosis unless patients expressed a higher NK cell gene signature (HR: 2.6, 95% CI: 1.2 - 5.9). (Figure 1D to F) In addition, the expression of *NT5E* correlated with NK cell gene signature in both sarcoma (r=0,321) and breast cancer tissues (r=0.326). On the contrary, we did not observe regulatory T cell gene signature to influence the prognostic value of *NT5E* expression. Notably, in sarcoma but not in breast cancer, *NT5E* expression significantly influenced the prognosis in patients with high but not low CD8 T cell signature (Hazard Ratio = 2.1, 95% Confidence Interval = 1.1 - 4.3) (Table 1). While the current understanding of CD73 as an immune checkpoint against tumor-infiltrating NK cells is not well understood, we show that the

prognostic value of *NT5E* gene expression is influenced by the NK cell signature expressed by different types of tumors.

Frequency of tumor-infiltrating CD73 positive NK cells correlates with larger tumor size in patients with breast cancer

To confirm the prognostic value of CD73 expression by tumor-infiltrating NK cells, peripheral blood and tumor resections were analyzed by flow cytometry from individual cohorts of breast cancer and sarcoma. Unlike peripheral blood NK cells and tumor-infiltrating T cells, tumor-infiltrating NK cells expressed significantly higher levels of cell surface CD73. (Figure 1G to I and Supplementary Figure 1A) Upon analysis of clinical characteristics, it was observed that the frequency of CD73+ NK cells correlated with breast tumors of larger size based on clinical TNM (tumor, node and metastasis) staging measurement cut-off (>5cm). (Table 2) and Figure 1J) Although not significant, triple negative breast cancer had a higher frequency of CD73+ NK cells while the frequency of total NK cells among CD45+ TILs was significantly higher in the luminal B subtype. (Supplementary Figure 1B and C) Importantly, the presence of CD73+ NK cells was independent of tumor CD73 expression or frequency of tumor-infiltrating NK cells. (Supplementary figure 1D and E). Taken together, these observations show that CD73+ NK cells were found only in the tumor microenvironment and that the frequency of these cells correlates with larger tumor size in patients with breast cancer.

CD73+ NK cells show increased expression of multiple immune checkpoint receptors.

To investigate whether CD73 is upregulated as a bona fide immune checkpoint,

flow cytometry analysis was performed to compare tumor-infiltrating NK cells and peripheral blood NK cells from patients with breast cancer and sarcoma for the multiple expression of other known immune checkpoints. (gating strategy shown in Supplementary Figure 2A) Using principal component analysis, a greater phenotypic heterogeneity within CD73+ tumor-infiltrating NK cells in contrast to peripheral blood NK cells and CD73- tumor-infiltrating NK cells was observed. (Figure 2A) The greatest proportion of the variability was attributed to surface expression of TIM-3 and LAG-3. (Supplementary Figure 2B) From analyzing the expression of different combinations of immune checkpoint receptors, we observed that CD73- subset of tumor-infiltrating NK cells do not co-express more than one immune checkpoint receptor. (Figure 2B) Similarly, t-SNE analysis showed distinct populations of CD73+ NK cells expressing multiple immune checkpoints. (Figure 2C) Unlike peripheral blood NK cells, tumor-infiltrating NK cells co-expressed other immune checkpoints including LAG-3, TIM-3, PD-1, VISTA and PD-L1. Furthermore, the expression of these immune checkpoints was significantly higher in CD73+ compared with CD73- tumor-infiltrating NK cells. (Figure 2D-G and Supplementary Figure 2C) Although the expression of PD-1 on CD73+ NK cells was significantly higher compared with CD73- NK cells, it was generally lower compared with other immune checkpoint receptors on both CD73- (mean=3.28%) and CD73+ (mean=9.50%) tumor-infiltrating NK cells. (Figure 2H) Analysis of the expression of activating receptors on tumor-infiltrating NK cells showed that the expression of NKG2C and NKp44 was significantly higher on CD73+ NK cells compared with CD73- NK cells. In contrast, the expression of NKG2D and NKp46 did not differ between CD73 + and CD73- tumor-infiltrating NK cells. (Supplementary Figure 2C-F). Collectively, NK cells from tumor resections, in

particularly the CD73+ cells, expressed a variable repertoire of immune checkpoints on their surface that were not observed in peripheral blood NK cells.

NK cells acquire CD73 surface expression upon engagement of 4-1BBL on tumor cells

Based on our observations that tumor-infiltrating NK cells with CD73 expression also co-expressed higher levels of immune checkpoints, we hypothesized that CD73 acquisition was caused by an activation response by NK cells. To understand how NK cells acquired the expression of CD73, peripheral blood NK cells from healthy individuals were co-cultured with fresh sarcoma and breast tumor resections and analyzed for their expression of CD73. Upon 4 hours of *in vitro* co-culture with different tumors isolated from patient samples, these NK cells indeed upregulate the expression of CD73 (Figure 3A and B). Similar results were reproduced upon co-culture with a panel of tumor cell lines. (Figure 3C) These observations were dependent on physical cell contact as NK cells did not acquire the expression of CD73 when co-cultured with tumor cells separated by transwell or treated with tumor-conditioned culture media. (data not shown)

Since it was recently shown that agonistic anti-CD137 (4-1BB) induces CD73 expression on tumor infiltrating T cells, we sought to investigate if 4-1BB engagement could play a role in the induction of CD73 on NK cells.(26) To test this, recombinant 4-1BB soluble ligand was added to co-cultures of NK cells and primary sarcoma cell lines. Following a 4-hour co-culture, a significant reduction of CD73 expression was observed in the presence of recombinant 4-1BB ligand compared with untreated controls. (Figure 3D) To further strengthen these

observations, CRISPR/Cas9 was used to knockout 4-1BBL in these patient-derived cell lines. Similarly, upon co-culture with 4-1BB ligand edited cell lines, the expression of CD73 of NK cells was significantly reduced. (Figure 3E) To exclude that the induction of CD73 does not result due to general activation, NK cells were cultured with the MHC class I deficient K562 cell line. While co-culture with K562 does activate NK cells, it did not induce CD73 upregulation unless modified to overexpress 4-1BBL. (Figure 3F) These results demonstrated that 4-1BB engagement can promote the induction of CD73 expression though we do not exclude the possibilities that other co-stimulatory receptors could be involved in this process.

NK cells acquire CD73 surface expression via actin polymerization-dependent exocytosis

Although we observed that 48 hours of IL-2 stimulation induced up to 1-2% surface expression of CD73, confocal imaging and intracellular flow cytometry staining revealed the presence of CD73 even in tumor-experienced CD73- NK cells. (Figure 4A and Supplementary Figure 3A) Based on quantification of CD73 fluorescence intensity, no significant differences in overall cellular CD73 fluorescence but only membrane CD73 were observed upon co-culture with 4-1BBL transfected K562 cells. (Figure 4B and 4C) Furthermore, confocal imaging showed that the expression of CD107a and CD73 did not co-localize. To test if exposure to tumor cells stimulated the transport of CD73 protein to the cell membrane, inhibitors of actin polymerization was added during co-culture of NK cells and tumor cells. Indeed, co-culture with peripheral blood NK cells and 4-1BBL-expressing K562 targets in the presence of either cytochalasin D, Latrunculin B or Jasplakinolide

resulted in a dose-dependent reduction of CD73 surface expression. (Figure 4D to F) As NK cells acquire higher surface CD73 expression in 4 hours of tumor co-culture compared with overnight co-culture (data not shown), we hypothesized that CD73 can be shed. Indeed, soluble CD73 was detected upon co-culture with 4-1BBL-transduced K562 cells. Furthermore, cytochalasin D inhibited the secretion of soluble CD73, confirming that actin polymerization was essential also for the secretion of CD73 by NK cells. (Figure 4G) To address if CD73 expression and shedding was due to NK cell degranulation or vesicular transport, NK cells were simultaneously stained for the degranulation and vesicle markers CD107a and CD63, respectively. Upon contact with 4-1BBL-transduced K562 cells, CD73 was mainly expressed on CD63+ NK cells. Degranulating NK cells (CD107a+) that lack surface CD63 expression did not express CD73. While blocking actin dynamics can downregulate both CD107a and CD63 expression, cells that are still positive for CD63 and negative for CD107a had reduced expression of surface CD73 with treatment of either Cytochalasin D or Latrunculin B during 4 hours of co-culture. (Supplementary Figure 3B and C) Collectively, these results show that NK cells express CD73 intracellularly and transport it to the cell surface, and extracellular space upon contact with tumor cells.

<u>CD73+ NK cells undergo transcriptional reprogramming to acquire suppressive functions</u>

To investigate if the CD73 receptor expressed by NK cells is functional, the capacity of purified CD73+ NK cells to hydrolyze AMP was measured. CD73 enzymatic activity was only detected in CD73+ NK cells despite no significant differences in CD73 levels between tumor-experienced NK cells and CD73+ T

cells. (Figure 5A) To address if CD73+ NK cells differ in their suppressive activity, purified NK cells were added to proliferating autologous CD4+ T cells. At an NK to T cell responder ratio of 1:10, CD73+ NK cells significantly reduced the proliferation of CD4 T cells compared with CD73- NK cells. (Figure 5B) Importantly, these assays were performed without the addition of exogenous AMP, suggesting that CD73+ NK cells may inhibit CD4 T cell proliferation through other mechanisms than the production of adenosine. To uncover such underlying mechanisms, CD73+ and CD73- NK cells were purified from tumor co-cultures and subjected to RNA sequencing. From 5 independent tumor co-cultures, results showed that a total of 524 genes (259 up and 265 down) were differentially expressed by more than 2-fold. (Figure 5C, Supplementary Figure 4A and Supplementary Table S2) When filtered for immune-related genes, CD73+ NK cells generally upregulated genes associated with immune activation, chemokines, *CSF1* (encoding M-CSF) and *CSF2* (encoding GM-CSF).(Figure 5D) In analyzing the top 100 upregulated genes, functional nodes mostly related to lymphocyte activation were identified. (Figure 5E) Of interest, CD73+ NK cells upregulated genes that are related to IL-10 production and granulocyte chemotaxis, both of which could potentially play a role in immune suppression.

To validate and substantiate our findings from these co-culture assays, we further isolated tumor infiltrating NK cells from two breast tumors and two sarcomas for gene expression analysis. Not only did these experiments confirm the upregulation of IL-10 gene expression but also that several known targets that can be regulated by the STAT3 transcription factor. Notably, cytolytic genes such as granzyme B (*GZMB*) and perforin (*PRF1*) were downregulated. (Supplementary Figure 4B)

Similar to the gene expression data generated from in vitro cultures, the presence of STAT3 binding motifs were examined 2000 base pairs upstream (5') of the transcriptional start site of 259 significantly upregulated genes. Of the genes, 256 were recognized in the JASPAR database. Of the 256 genes identified, 61 genes with STAT3 binding motifs were identified. From these, genes with binding motifs for HIF1, CREB1 and NFKB which are all known to dimerize with STAT3 for transcriptional regulation were identified. (Supplementary Figure 4C) Together, gene expression analysis from both in vitro co-culture and tumor-infiltrating NK cells suggested STAT3 as a key regulator for transcriptional reprogramming of these CD73+ NK cells to acquire a regulatory phenotype.

CD73+ NK cells upregulate IL-10 and TGF-β production via STAT3 transcriptional activity

Since STAT3 is known to have immunoregulatory capacity and also regulates CD73 expression (27, 28), we sought to further investigate the role of STAT3 activity in these inducible CD73+ regulatory NK cells. We found that CD73+ NK cells displayed increased phosphorylation of serine residue 727 and tyrosine residue 705 of STAT3 as compared with CD73- NK cells. (Supplementary Figure 5A and B) To confirm if STAT3 is involved in inducing CD73+ immunoregulatory NK cells, the selective STAT3 inhibitor GPB730 was added to NK-tumor co-cultures. (Supplementary Figure 5C) (29, 30) During tumor co-culture, GPB730 decreased STAT3-S727 phosphorylation in NK cells while no significant changes in Y705 phosphorylation were observed. (Supplementary Figure 5D and E) Treatment with GPB730 prior to and during overnight tumor co-culture resulted in an average 3-fold (SD=1.19) reduction of the expression of CD73 on NK cells. (Figure 6A)

Since IL-10 was upregulated in both gene and protein levels by tumor-infiltrating CD73+ NK cells (Supplementary Figure 4B and Supplementary Figure 5F), NK cells were co-cultured with tumors cells and assayed for their production of IL-10. Indeed, upon co-culture with tumor cells, a significant upregulation of IL-10 production by CD73+ NK cells compared with CD73- NK cells were observed. In addition, CD73+ NK cells also produced higher levels of TGF-β compared with CD73- NK cells, and the capacity of CD73+ NK cells to produce these two cytokines was significantly reduced in the presence of GPB730. In addition, the production of TGF-β was significantly inhibited only at high doses of GPB730 during co-culture, whereas IL-10 production was inhibited by pre-treating NK cells with a low dose of GPB730. (Figure 6B and C) Next, NK cells were treated with GPB730 prior to tumor co-culture and tested for their ability to suppress CD4 T cells to produce IFNγ and proliferate. Compared with CD73- NK cells, CD73+ NK cells significantly suppressed CD4 T cell activity. Upon pre-treatment with GPB730, a significantly reduced suppression by NK cells was observed as evidenced by reduced $CFSE^{high}/IFN\gamma^{neg}$ CD4 T cell population. (Figure 6D-F)

Since GPB730 pre-treated NK cells showed reduced suppression of CD4 T cell IFNγ production (Figure 6G), we further investigated if either production of IL-10 or TGFβ was the direct underlying suppressive mechanism of CD4 T cells by CD73+ NK cells. Suppression assays performed in the presence of neutralizing antibodies to IL-10 restored the production of IFNγ by CD4 T cells, whereas the presence of the TGF-β1 receptor inhibitor Galunisertib did not. (Figure 6H and 6I) These results show that CD73+ NK cells upregulate STAT3 activity due to immune activation resulting in the production IL-10 that inhibits IFNγ production by CD4 T cells.

Discussion

Under physiological conditions, purinergic receptors play an important role for lineage commitment, tissue repair, as well as to confer immune tolerance. (2, 31) However, extracellular adenosine could be dysregulated by CD73-overexpressing tumors contributing to resistance against cytostatic drugs and immune therapies.(7, 26, 32, 33) Despite the extensive efforts to introduce CD73 inhibitors into the clinic, the complexity in the regulation of this ectonucleotidase is not well understood.(34) We observed that the predictive value of tumor *NT5E* expression could be influenced by the magnitude of the NK cell gene signature in breast cancer and sarcoma. Notably, the expression of *NT5E* influenced the prognosis of breast cancer and sarcoma patients with low and high NK cell gene signatures respectively. The underlying mechanisms of these findings are however unclear.

Since sarcomas are mesenchymal tumors and breast cancers are epithelial tumors, their respective influence on NK cell infiltration and activity may differ. While a positive correlation between tumor *NT5E* expression and NK cell gene signature was observed, CD73 was also found to be expressed on tumor infiltrating NK cells. The proportion of CD73+ tumor infiltrating NK cells also positively correlated with larger breast tumors.

While regulatory T cells have been shown to express the ectonucleotidases CD39 and CD73 and inhibit T cell responses via the production of adenosine (35), less is known regarding the expression of these ectonucleotidases in conventional T cells as well as NK cells. Upon exposure to mesenchymal stem cells (MSCs), T cells upregulate CD39 resulting in suppression of activated T cells via increased production of extracellular adenosine. (36) Similarly, studies reported that NK cells acquire the expression of CD73 after physical contact with human umbilical cord-derived MSCs or dental pulp stem cells. (37, 38) In cancer, NK cells from gastrointestinal stromal tumors (GISTs) have been found to express higher levels of surface CD73. (39) Yet, the current understanding of tumor infiltrating NK cells is unclear with regards to their robustness in phenotype and function. Here we extend these observations and demonstrate that NK cells not only upregulate the expression of CD73 but also several other immune checkpoint receptors implicating immune exhaustion. We found that these NK cells underwent transcriptional reprogramming to acquire non-canonical functions to suppress the immune environment.

The basis of our study was to co-culture activated NK cells with tumor cells to model tumor-experienced NK cells within the TME. Upon physical contact with tumor cells, a rapid cell-surface expression and secretion of CD73 by NK cells via vesicular transport was observed. This observation was not restricted to tumor cell contact as we also observed that endothelial cells and fibroblasts could also induce CD73 expression on NK cells. (data not shown) While agonizing 4-1BB activates both CD4 and CD8 T cells in vitro, engaging 4-1BB can result in an impaired NK cell development and induce cell death in resting NK cells. (40-42) Mechanistically, 4-1BB stimulation was involved in the induction of CD73, which was also previously studied in tumor infiltrating T cells.(26) Given that there could be other chronic stimulation involved in the generation of CD73+ NK cells within the TME, there could be other potential underlying mechanisms left uncovered. Considering that prior studies have demonstrated that CTLA-4 and CD73 can be stored within intracellular vesicles, we hypothesized and demonstrated that exocytosis was involved in the underlying mechanism in which NK cells acquire CD73 expression. (35, 43, 44) While CD73 is an enzyme that hydrolyses extracellular AMP on the cell surface, we also showed that these tumor-experienced NK cells could also shed CD73 protein into the extracellular space - a finding that might have clinical relevance since soluble CD73 has been suggested to be a biomarker in patients with metastatic cancer. (45) Another possibility that we did not explore was if these NK cells could secrete exosomes expressing CD73 which was previously found to be upregulated in serum from patients with head and neck squamous cell carcinoma. (35, 46)

The concept of regulatory NK cells is controversial. An early study demonstrated that NK cells become immunosuppressive and produce IL-10 during acute infection. (22) Later it was reported that $CD56^{bright}$ NK cells not only serve as regulatory cells secreting IL-10 but also synthesize adenosine via the CD38/PC1-CD73 pathway.(21) A recent study by Crome et. al. showed that CD56+CD3- regulatory innate lymphoid cells express higher levels of NKp46 with elevated IL-22 production. (23) Without the assumption that these cells are NK cells, the group demonstrated that this unique population of innate lymphoid cells (ILCs) suppresses the ex-vivo expansion of TILs from high-grade serous cancers.

By studying how tumor cells can influence normal NK cells to acquire CD73, we demonstrated that CD73+ NK cells suppress both proliferation and cytokine production of CD4 T cells as compared to CD73- NK cells. Although the induced CD73 receptor on NK cells was functional as evidenced by the ability to hydrolyze AMP, the addition of exogenous AMP did not influence the immune suppression mediated by CD73+ NK cells (data not shown). Likewise, adenosine receptor inhibitors did not significantly change the ability of CD73+ NK cells to suppress CD4 T cell responses (data not shown). Thus, we hypothesize that CD73+ NK cells may suppress CD4 T cells via mechanisms other than the production of extracellular adenosine. While studies have shown that NK cells can produce IL-10 via binding of Ly49H or IL-12 stimulation in viral and systemic infections respectively, we found that tumor-experienced NK cells produced IL-10 via STAT3 activation. (22, 47) It was recently shown that STAT3 negatively regulates several NK cell functions and drives the expression of PD-L1. (48, 49) Our results support

that STAT3 drives the generation of CD73+ regulatory NK cells as well as the production of IL-10 by these NK cells.

In summary, NK cells undergo dynamic phenotypic and functional changes influenced by different cues within the heterogeneous TME. It is plausible to envision that future investigations on regulatory NK cells could potentially correlate with other undesirable clinical outcomes in a variety of solid tumors. Our results also supported the use of STAT3 and IL-10 inhibitors by dampening the suppressive tumor immune landscape and thereby complement current immunotherapies.

Methods

Cell lines

Commercial cell lines used for co-cultures are 786O, CAKI2, MDAMB231, MDAMB436 and K562. (American Type Culture Collection) K562 transduced with 4-1BB ligand were kindly provided by Dr. Crystal Mackall, National Cancer Institute, Bethesda. Patient-derived sarcoma cell lines established from surgical resections of patient 8 and 9 listed in table 3. In brief, whole tumor was digested and processed. (Tumor Dissociation Kit, Miltenyi) Tumor cells were then isolated by negative selection. (Tumor cell isolation kit, Miltenyi) Adherent cells were passaged at least 5 times before being used for experiments. All cell lines were maintained in RPMI1640 or in DMEM (ThermoFisher Scientific) supplemented with 10% fetal bovine serum. (ThermoFisher Scientific).

Chemicals

Cytochalasin D, Latrunculin B and Jasplakinolide (Sigma Aldrich) was used to inhibit actin polymerization in tumor co-cultures. To inhibit STAT3, the selective small molecule inhibitor GPB730 *(N*-[(4R,7R,9R, 11S)- 11-hydroxy-9-methyl-2-oxo-3-oxatricyclo [5.3.1.$0^{4,11}$] undec-l(10)-en-9-yl-4-methylbenzene-l-sulfonamide]) was used. (See supplementary Figure 5C for chemical structure) GPB730 and the inhibitor for TGF-β type 1 receptor, Galunisertib (Selleckchem) was used for co-cultures and suppression assays. Recombinant 4-1BB was used for co-cultures to block 4-1BBL engagement. (Cat no. 310-15, PeproTech)

CRISPR-knockout of CD137L in Patient-derived Cell Lines

To generate sarcoma cells with a knockout of CD137L, gRNAs were designed to bind within exon 1 of the gene using the CRISPOR algorithm. (50) The gRNA (ATACGCCTCTGACGCTTCAC) was cloned into the lentiviral expression vector lentiCRISPR v2 using Esp3I insertion sites. (51) Plasmids were verified by sequencing. Lentivirus was produced as previously described.(52) Briefly, $1x10^6$ HEK293FT cells were plated into a poly-D-lysine-coated 60-mm dish (BD Biosciences). The following day, the cells were transfected with 4.8μg of the cloned lentiCRISPR v2 containing the gRNA, 2.4μg of pMDLg/pRRE (Addgene, Cambridge, MA), 1.6μg of pRSV-REV (Addgene), and 0.8μg of phCMV-VSV-G (Addgene) using calcium phosphate transfection kit (Sigma- Aldrich) in the presence of 25μM chloroquine (Sigma Aldrich). At 16 hours after transfection, the medium was changed, and the virus particles were collected after an additional 28h, by filtering the supernatant through a 0.45μm filter and stored at -80°C. 15000 sarcoma cells suspended in 2ml of RPMI medium supplemented with 10% FBS, were transduced with 500μl of virus-containing supernatant for 8 hours in 8μg/ml protamine sulfate (Sigma Aldrich). After transduction, cells were cultured for 14 days and then sorted for absent staining with CD137L antibody (Cat no. 311503, Biolegend) by using fluorescence-activated cell sorting (FACS) with BDARIA Fusion. (BD Biosciences) Sorted cells were seeded overnight in culture before co-culture experiments.

NK cell isolation and culture

Peripheral blood mononuclear cells (PBMC) were collected after Ficoll gradient centrifugation (GE Healthcare). NK cells were isolated by negative selection based on the manufacturer's protocol. (Human NK cells isolation kit, Miltenyi) Isolated NK

cells were then cultured in X-vivo20 (Lonza) supplemented with 10% human AB serum (Karolinska University Hospital Blood Bank) with 1000IU/mL of IL-2 for 48 hours. (Proleukin) In the absence of IL-2, NK cells were co-cultured with tumor cell lines for 4 or 16 hours before cell sorting and FACS analysis.

CD4 T Cell Isolation and Suppression Assay

CD4 T cells were isolated by negative selection based on the manufacturer's protocol. (Human CD4 T cells isolation kit, Miltenyi) Isolated CD4 T cells were labelled with 1μM of CFSE (Biolegend) and stimulated with 12μL/million cells of CD3/CD28 beads (ThermoFisher Scientific) and 50 IU/mL of IL-2 for 48 hours prior to suppression assay. For the suppression assay, CD73+ and CD73- NK cells were isolated by flow cytometry sorting and co-cultured with autologous activated CD4 T cells at a suppressor to responder ratio of 1:10 in serum free X-vivo20 media. FACS analysis was performed after 48 hours of co-culture.

Flow Cytometric Analysis

Single cell suspensions of PBMC and tissue samples were washed with FACS buffer (5% FBS in PBS) before staining with antibody mix (See Supplementary Table S3) in the presence of Human Fc Block™ (BD Biosciences). All samples were acquired on Novocyte (ACEA Biosciences). All data were analyzed with FlowJo software (Tree Star). FCS files with only NK cells were concatenated with FlowJo for downstream tSNE analysis. PCA analysis was performed by SIMCA 15 software. (Umetrics) For staining of IFNγ, cells were incubated for 1 hour, 37°C with 100ng/ml of Phorbol Myristate Acetate (PMA) and 1μg/ml of ionomycin (Sigma Aldrich) in X-vivo20 media supplemented with 10% hAB. After 1 hour, GolgiSTOP

and GolgiPLUG (BD Biosciences) were used in combination according to the manufacturer's protocol. Cells were then further incubated for 3 hours under the same conditions before cell surface staining. After fixation and permeabilization, antibodies against IFNγ were added for intracellular staining at room temperature for 20 minutes before cells were washed and acquired on Novocyte. See Supplementary Table S3 for antibody panel. For IL-10 and TGF-β staining, GolgiSTOP and GolgiPLUG (BD Biosciences) were used in combination for 24 hours within the tumor co-culture setting. Surface and intracellular cytokine staining was then performed as described above. For staining of phosphorylated STAT3, cells were fixated with Fix Buffer I (BD Biosciences) at 37 ºC for 10 minutes. Permeabilization of cells was done by resuspension in ice-cold Perm Buffer III (BD) for 45 minutes at 4 ºC. After permeabilization and washing, cells were stained with anti-STAT3 pY705 and anti-STAT3 pS727 (BD Biosciences) diluted 1:100 in FACS buffer for 1 hour at 4 ºC. Cells were washed twice in FACS buffer before acquisition on flow cytometer.

CD73 ELISA and Enzymatic Activity Assay

NK cells ($0.5X10^6$) were co-cultured with $0.1X10^6$ of 4-1BBL transduced K562 cells for 24 hours at an NK to K562 ratio of 5:1. Following co-culture, supernatants were collected to detect CD73 by ELISA based on the manufacturer's protocol. (Nordic Biosite) To test the enzymatic activity of CD73, a modified AMP depletion assay was used. (53) Briefly, 5000 sorted CD73+ and CD73- T and NK cells were seeded in each well of 96-well plate in serum free X-vivo20 media with 0.4mM of AMP (Sigma Aldrich). Cells were incubated for 90 minutes at 37°C, 5% CO2. After incubation, 25uL of cell supernatant was collected and mixed with 25uL of X-vivo20

media with 200uM of ATP (Sigma Aldrich). The mixture was then added in a white-bottom plate with Cell-Titer Glo reagent (Promega) at 1:1 ratio. Luminescence readout was obtained with an integration time of 100ms on SPARK^{TM} 10M plate reader (TECAN). Raw values from CD73- cell controls were used to subtract background signals.

STAT3 reporter gene assay

Dose response activity to determine IC50 at eight different doses in triplicate was used in a STAT3 reporter system. Briefly, the STAT3 reporter/HEK293 cell line was plated in 96-well white plates for 16 h. Cells were pretreated with GPB730 for 1 h. Cells were then treated with IL-6 to induce STAT3 activation for 16 h. Luciferase activity was measured and analyzed.

Confocal Image Analysis

Cells were seeded and incubated for 20 minutes on slides coated with an ICAM-1 (BioLegend, #552904) solution at 1µg/ml for 1 hour at 37°C. Cells were then fixed using 4% paraformaldehyde for 20 minutes before being permeabilized with a 0.1% triton solution for 10 minutes. Blocking was performed using 5%FBS in PBS for 1 hour. The cells were thereafter stained using mouse anti-human CD73 antibody (Invitrogen, 41-0200, 1/100) for 1 hour before incubation with the secondary antibody goat anti-Mouse IgG conjugated with AlexaFluor647 (Invitrogen, A-21236, 1/500) for 1 hour. Cells were thereafter incubated with biotinylated mouse anti-human 63 (abcam, ab134331, 1/200) for 1 hour or biotinylated mouse anti-human 107a (BioLegend, 328604, 1/100) for 1 hour. Finally, the cells were incubated with a solution containing DAPI (1/100), AlexaFluor 488 Phalloidin (Invitrogen, A12379,

1/200) and AlexaFluor 555 streptavidin (Invitrogen, S21381, 1/500) for 30 minutes. The cells were then mounted in ProLong Diamond Antifade Mountant (Invitrogen, P36965). The cells were imaged using a Zeiss LSM800 confocal microscope equipped with Plan-Apochromat 63x/1.40 Oil DIC M27 lens and analysis was performed using FIJI/ImageJ and CellProfiler.

Gene Expression Analysis of NK cells after Tumor Co-culture

Following 4 hours of co-culture with 786O tumor cell line and NK cells (n=5) FACS-sorted CD73+ and CD73- NK cells were used to isolate RNA using RNAeasy microkit based on the manufacturer's protocol. (Qiagen) Total RNA integrity was analyzed using the Agilent 2100 Bioanalyzer RNA 6000 Pico Kit and quantified on the Qubit 3.0 Fluorometer using the Qubit RNA High Sensitivity Assay Kit or by real-time PCR using Applied Biosystems' RNA Quantification Kit on the Agilent AriaMx. Total RNA was normalized to 28 picograms of input for full-length cDNA generation using Takara's SMART-Seq v4 Ultra Low Input RNA Kit following the manufacturer's recommendations. cDNA was normalized to 1 nanogram of input for sequencing library generation using Illumina's Nextera XT DNA Library Preparation Kit following the manufacturer's protocol. cDNA libraries were quantified by qPCR using Kapa Biosystems' Library Quantification Kit on the Roche LightCycler 480 Instrument II following the manufacturer's protocol. cDNA libraries were normalized to 1.5-2 nM, pooled and denatured following Illumina's NextSeq System Denature and Dilute Libraries Guide. Final pooled libraries (n=5 samples) were spiked with 1% PhiX as an internal control and loaded at a final concentration of 1.6 pM onto the Illumina NextSeq 500 platform. cDNA libraries were sequenced on a 2x75 bp paired-end run using the NextSeq 500 High Output

v2 Kit (150 cycles) for n=2 sequencing runs. Approximately 763 million indexed pass filter paired-end reads were generated during sequencing run 1 and ~760 million indexed, pass filter paired-end reads were generated during sequencing run 2.

Raw data were uploaded on Partek Flow for data analysis and GEO repository (GSE125119). Raw reads were quality trimmed based on a minimum Phred quality score of 20 and aligned to human genome assembly GRCh38 (hg38) using STAR v2.5.3a with default parameters. Gene level counts were normalized using CPM (counts per million) and quantified using a mixed-model ANOVA to account for donor ID as a random effect and CD73+/- expression status as a fixed factor. 8456 differentially expressed genes were identified (See Supplementary Table S1) while 524 were significantly differentially expressed (p-value $\leq$0.05; Fold Change +/-2; See Supplementary Table S2). A volcano plot (Figure 5C) was generated to visualize the significance and the magnitude of changes in gene expression. From the filtered 524 genes (Supplementary Table S2), 74 immune-related genes were identified from Gene Ontology Database; a heatmap was generated using (unsupervised) hierarchical clustering (average linkage distance metric and Euclidean point distance metric) (Figure 5D). Note binning of genes in the X-axis for display purposes.

Gene ontology enrichment analysis was done based on the top 100 genes upregulated (See Supplementary Table S2) with ClueGO plugin in Cytoscape. Using default Cluego settings and GO term fusion, the 100 gene IDs were submitted to query the GO-Biological process database (EBI, QuickGO, 15783

terms associated to 17268 unique genes, updated on 11/20/2017). Gene ontology terms are presented as nodes and clustered together based on the term similarity. (Figure 5E) From supplementary table S2, 266 significantly upregulated genes were uploaded on oPOSSUM-3 to query for STAT3 transcription binding site up to -2000 base pairs upstream.

Gene Expression Analysis of Tumor Infiltrating NK cells

Prior to FACS sorting, immune cells were enriched from freshly processed tumor samples. (CD45 isolation kit, Miltenyi) Based on CD73 expression, NK cells were sorted directly to lysis buffer for RNA extraction. (RNAeasy microkit, Qiagen) A total amount of 1 μg RNA per sample was used as input material for the RNA sample preparations. Sequencing libraries were generated using NEBNext® Ultra TM RNA Library Prep Kit for Illumina® (New England Biolabs) following manufacturer's recommendations and index codes were added to attribute sequences to each sample. In order to select cDNA fragments of preferentially 150~200 bp in length, the library fragments were purified with AMPure XP system (Beckman Coulter). Then 3 μl USER Enzyme (NEB, USA) was used with size-selected, adaptor ligated cDNA at 37 °C for 15 min followed by 5 min at 95 °C before PCR. PCR was performed with Phusion High-Fidelity DNA polymerase, Universal PCR primers and Index (X) Primer. At last, PCR products were purified (AMPure XP system) and library quality was assessed on the Agilent Bioanalyzer 2100 system. The clustering of the index-coded samples was performed on a cBot Cluster Generation System using PE Cluster Kit cBot-HS (Illumina) according to the manufacturer's instructions. After cluster generation, the library preparations were sequenced on an Illumina platform and paired-end reads were generated.

Reference genome and gene model annotation files were downloaded from genome website browser (NCBI/UCSC/Ensembl) directly. Paired-end clean reads were mapped to the reference genome using HISAT2 software. Prior to differential gene expression analysis, for each sequenced library, the read counts were adjusted by edgeR program through one scaling normalized factor. Differential expression analysis of two conditions was performed using the DEGseq R package. p-Values were adjusted using the Benjamini and Hochberg methods.

Application of an NK cell signature to public datasets

Normalized, batch corrected, RNA-sequencing data and patient/tumor clinico-pathological characteristics from the Pan-Cancer Genome Atlas project (Pan-Can) were accessed from NIH genomic data commons (GDC) database (https://gdc.cancer.gov). Genes representing the NK signature (*KLRB1, CD160, NCR1, NCR3, PRF1*) were extracted from the dataset and their expression summed on a per tumor (column wise) basis to generate an NK signature score. Signatures for CD8 cytotoxic T cells (*CD3E, CD8A*) and regulatory T cells (*FOXP3*) were derived using the same scoring method. (25) For breast tumor and sarcoma specific analyses this score was divided into quartiles within each cancer type and the expression of the *NT5E* gene was examined within the highest and lowest NK signature quartiles. Results were tabulated in table 1.

Statistics

Kaplan-Meier analysis was performed using the *survival* and *survplot* R packages with *NT5E* split into a binary (Low/High) variable based on the median value and with Progression Free Interval as the survival endpoint. Permutation test shown in

supplementary figure 2 was performed using SPICE version 6.0 software (National Institutes of Health). All other experimental data were plotted and tested for significance on Prism 8.0 (Graphpad software) as described in figure legends unless stated otherwise. P values below 0.05 were considered as significant. All error bars represent standard deviation of the mean.

Study Approval

Tumor resections were obtained from breast cancer patients at Karolinska University Hospital, St Göran Hospital and Stockholm South General Hospital. (Table 2) All cases except case 17 are untreated primary tumors. Tumor resections and peripheral blood were collected from sarcoma patients at Karolinska University Hospital. (Table 3) Prior to resection, informed consent was given and the collections of patient samples were approved by the ethical review board of Karolinska Institutet (#2012/90-31/2, #2013/1979-31, #2016/957-31 and #2017/742-32) and in accordance with the Declaration of Helsinki. Peripheral blood samples were obtained from purchased anonymized by-products of blood donations from healthy adult donors at the Karolinska University Hospital Blood Bank.

Author Contributions

NSY, RJ, TNP, BE, AJ, HJ, and LA contributed to the study conception and design. NSY, YY, RJ, MR, CX, CZ, WA, MS, AE, JM, WL, HF, HJ, and LA contributed to the development of research methodology. NSY, YY, RJ, MR, CX, CZ, TNP, BE, SC, TR, WA, contributed to the acquisition of data and conducted experiments. NSY, YY, TNP, BE, AJ, dBJ, BJ, CR, JM, WL, HF, HJ, and LA contributed to data

analysis and interpretation, and essential reagents. NSY, RJ, WA, TNP and LA, contributed to the writing the manuscript.

Acknowledgements

We thank Maria Johansson and Juan Basile at the Biomedicum Flow Cytometry Core Facility, Karolinska Institute. We thank Marissa Brooks at the Genomics Core Facility and Kim Kusser at the Flow Cytometry Facility at the Center for Collaborative Research, Nova Southeastern University. We thank Dr. Chris Tibitt, Apple Tay Hui Min and Anna Malmerfelt, Karolinska Institute, for technical assistance. This work was supported by the Swedish Cancer Society #CAN 2015/421 and #CAN 2018/451), the Swedish Childhood Cancer Foundation (#PR PR2014-0093 and PR2017-0049) and the Cancer Research Foundations of Radiumhemmet (161192 and 181183), Vinnova Swelife and Medtech4Health (#2018-00262), and The Sagen Foundation.

References

1. Allard B, Longhi MS, Robson SC, and Stagg J. The ectonucleotidases CD39 and CD73: Novel checkpoint inhibitor targets. *Immunological reviews.* 2017;276(1):121-44.
2. Scarfi S. Purinergic receptors and nucleotide processing ectoenzymes: Their roles in regulating mesenchymal stem cell functions. *World J Stem Cells.* 2014;6(2):153-62.
3. Allard D, Allard B, Gaudreau PO, Chrobak P, and Stagg J. CD73-adenosine: a next-generation target in immuno-oncology. *Immunotherapy.* 2016;8(2):145-63.
4. Hausler SF, Del Barrio IM, Diessner J, Stein RG, Strohschein J, Honig A, et al. Anti-CD39 and anti-CD73 antibodies A1 and 7G2 improve targeted therapy in ovarian cancer by blocking adenosine-dependent immune evasion. *Am J Transl Res.* 2014;6(2):129-39.
5. Antonioli L, Yegutkin GG, Pacher P, Blandizzi C, and Hasko G. Anti-CD73 in cancer immunotherapy: awakening new opportunities. *Trends Cancer.* 2016;2(2):95-109.
6. Stagg J, Divisekera U, McLaughlin N, Sharkey J, Pommey S, Denoyer D, et al. Anti-CD73 antibody therapy inhibits breast tumor growth and metastasis. *Proc Natl Acad Sci U S A.* 2010;107(4):1547-52.
7. Loi S, Pommey S, Haibe-Kains B, Beavis PA, Darcy PK, Smyth MJ, et al. CD73 promotes anthracycline resistance and poor prognosis in triple negative breast cancer. *Proc Natl Acad Sci U S A.* 2013;110(27):11091-6.
8. Astra Zeneca. Phase II Umbrella Study of Novel Anti-cancer Agents in Patients With NSCLC Who Progressed on an Anti-PD-1/PD-L1 Containing

Therapy. (HUDSON) Available from: https://ClinicalTrials.gov/show/NCT03334617.

9. MedImmune LLC. Oleclumab (MEDI9447) EGFRm NSCLC Novel Combination Study. Available from: https://ClinicalTrials.gov/show/NCT03381274.

10. MedImmune LLC. MEDI9447 (Oleclumab) Pancreatic Chemotherapy Combination Study. Available from: https://ClinicalTrials.gov/show/NCT03611556.

11. MedImmune LLC. MEDI9447 Alone and in Combination With MEDI4736 in Adult Subjects with Select Advanced Solid Tumors. Available from: https://ClinicalTrials.gov/show/NCT02503774.

12. Gettinger S, Choi J, Hastings K, Truini A, Datar I, Sowell R, et al. Impaired HLA Class I Antigen Processing and Presentation as a Mechanism of Acquired Resistance to Immune Checkpoint Inhibitors in Lung Cancer. *Cancer Discovery.* 2017;7(12).

13. Dahlberg CI, Sarhan D, Chrobok M, Duru AD, and Alici E. Natural Killer Cell-Based Therapies Targeting Cancer: Possible Strategies to Gain and Sustain Anti-Tumor Activity. *Front Immunol.* 2015;6:605.

14. Karre K. Natural killer cell recognition of missing self. *Nat Immunol.* 2008;9(5):477-80.

15. Vivier E, Tomasello E, Baratin M, Walzer T, and Ugolini S. Functions of natural killer cells. *Nat Immunol.* 2008;9(5):503-10.

16. Long EO, Kim HS, Liu D, Peterson ME, and Rajagopalan S. Controlling natural killer cell responses: integration of signals for activation and inhibition. *Annu Rev Immunol.* 2013;31:227-58.
17. Larsen SK, Gao Y, and Basse PH. NK cells in the tumor microenvironment. *Crit Rev Oncog.* 2014;19(1-2):91-105.
18. Tian W, Wang L, Yuan L, Duan W, Zhao W, Wang S, et al. A prognostic risk model for patients with triple negative breast cancer based on stromal natural killer cells, tumor-associated macrophages and growth-arrest specific protein 6. *Cancer Science.* 2016;107(7):882-9.
19. Guillerey C, Huntington ND, and Smyth MJ. Targeting natural killer cells in cancer immunotherapy. *Nat Immunol.* 2016;17(9):1025-36.
20. Morvan MG, and Lanier LL. NK cells and cancer: you can teach innate cells new tricks. *Nat Rev Cancer.* 2016;16(1):7-19.
21. Morandi F, Horenstein AL, Chillemi A, Quarona V, Chiesa S, Imperatori A, et al. CD56brightCD16- NK Cells Produce Adenosine through a CD38-Mediated Pathway and Act as Regulatory Cells Inhibiting Autologous CD4+ T Cell Proliferation. *J Immunol.* 2015;195(3):965-72.
22. Vivier E, and Ugolini S. Regulatory natural killer cells: new players in the IL-10 anti-inflammatory response. *Cell Host Microbe.* 2009;6(6):493-5.
23. Crome SQ, Nguyen LT, Lopez-Verges S, Yang SY, Martin B, Yam JY, et al. A distinct innate lymphoid cell population regulates tumor-associated T cells. *Nat Med.* 2017;23(3):368-75.
24. Jiang T, Xu X, Qiao M, Li X, Zhao C, Zhou F, et al. Comprehensive evaluation of NT5E/CD73 expression and its prognostic significance in distinct types of cancers. *BMC Cancer.* 2018;18(1):267.

25. Bottcher JP, Bonavita E, Chakravarty P, Blees H, Cabeza-Cabrerizo M, Sammicheli S, et al. NK Cells Stimulate Recruitment of cDC1 into the Tumor Microenvironment Promoting Cancer Immune Control. *Cell.* 2018;172(5):1022-37 e14.

26. Chen S, Fan J, Zhang M, Qin L, Dominguez D, Long A, et al. CD73 expression on effector T cells sustained by TGF-beta facilitates tumor resistance to anti-4-1BB/CD137 therapy. *Nat Commun.* 2019;10(1):150.

27. Chalmin F, Mignot G, Bruchard M, Chevriaux A, Vegran F, Hichami A, et al. Stat3 and Gfi-1 transcription factors control Th17 cell immunosuppressive activity via the regulation of ectonucleotidase expression. *Immunity.* 2012;36(3):362-73.

28. Hedrich CM, Rauen T, Apostolidis SA, Grammatikos AP, Rodriguez Rodriguez N, Ioannidis C, et al. Stat3 promotes IL-10 expression in lupus T cells through trans-activation and chromatin remodeling. *Proc Natl Acad Sci U S A.* 2014;111(37):13457-62.

29. Don-Doncow N, Escobar Z, Johansson M, Kjellstrom S, Garcia V, Munoz E, et al. Galiellalactone is a direct inhibitor of the transcription factor STAT3 in prostate cancer cells. *J Biol Chem.* 2014;289(23):15969-78.

30. Escobar Z, Bjartell A, Canesin G, Evans-Axelsson S, Sterner O, Hellsten R, et al. Preclinical Characterization of 3beta-(N-Acetyl l-cysteine methyl ester)-2abeta,3-dihydrogaliellalactone (GPA512), a Prodrug of a Direct STAT3 Inhibitor for the Treatment of Prostate Cancer. *J Med Chem.* 2016;59(10):4551-62.

31. MacDonald GI, Augello A, and De Bari C. Role of mesenchymal stem cells in reestablishing immunologic tolerance in autoimmune rheumatic diseases. *Arthritis Rheum.* 2011;63(9):2547-57.
32. Streicher K, Higgs BW, Wu S, Coffman K, Damera G, Durham N, et al. Increased CD73 and reduced IFNG signature expression in relation to response rates to anti-PD-1(L1) therapies in EGFR-mutant NSCLC. 2017;35(15_suppl):11505-.
33. Inoue Y, Yoshimura K, Kurabe N, Kahyo T, Kawase A, Tanahashi M, et al. Prognostic impact of CD73 and A2A adenosine receptor expression in non-small-cell lung cancer. *Oncotarget.* 2017;8(5):8738-51.
34. Garber K. Adenosine checkpoint agent blazes a trail, joins immunotherapy roster. *Nature biotechnology.* 2017;35(9):805-7.
35. Schuler PJ, Saze Z, Hong CS, Muller L, Gillespie DG, Cheng D, et al. Human CD4+ CD39+ regulatory T cells produce adenosine upon co-expression of surface CD73 or contact with CD73+ exosomes or CD73+ cells. *Clin Exp Immunol.* 2014;177(2):531-43.
36. Saldanha-Araujo F, Ferreira FI, Palma PV, Araujo AG, Queiroz RH, Covas DT, et al. Mesenchymal stromal cells up-regulate CD39 and increase adenosine production to suppress activated T-lymphocytes. *Stem Cell Res.* 2011;7(1):66-74.
37. Chatterjee D, Tufa DM, Baehre H, Hass R, Schmidt RE, and Jacobs R. Natural killer cells acquire CD73 expression upon exposure to mesenchymal stem cells. *Blood.* 2014;123(4):594-5.
38. Yan F, Liu OS, Zhang HX, Zhou YY, Zhou D, Zhou ZK, et al. Human dental pulp stem cells regulate allogeneic NK cells' function via induction of anti-

inflammatory purinergic signalling in activated NK cells. *Cell Proliferat.* 2019;52(3).

39. Vijayan D, Barkauskas DS, Stannard K, Sult E, Buonpane R, Takeda K, et al. Selective activation of anti-CD73 mechanisms in control of primary tumors and metastases. *Oncoimmunology.* 2017;6(5):e1312044.

40. Niu L, Strahotin S, Hewes B, Zhang B, Zhang Y, Archer D, et al. Cytokine-mediated disruption of lymphocyte trafficking, hemopoiesis, and induction of lymphopenia, anemia, and thrombocytopenia in anti-CD137-treated mice. *J Immunol.* 2007;178(7):4194-213.

41. Choi BK, Kim YH, Kim CH, Kim MS, Kim KH, Oh HS, et al. Peripheral 4-1BB signaling negatively regulates NK cell development through IFN-gamma. *J Immunol.* 2010;185(3):1404-11.

42. Vinay DS, Cha K, and Kwon BS. Dual immunoregulatory pathways of 4-1BB signaling. *J Mol Med (Berl).* 2006;84(9):726-36.

43. Schneider H, and Rudd CE. Diverse mechanisms regulate the surface expression of immunotherapeutic target ctla-4. *Front Immunol.* 2014;5:619.

44. Smyth LA, Ratnasothy K, Tsang JY, Boardman D, Warley A, Lechler R, et al. CD73 expression on extracellular vesicles derived from CD4+ CD25+ Foxp3+ T cells contributes to their regulatory function. *Eur J Immunol.* 2013;43(9):2430-40.

45. Morello S, Capone M, Sorrentino C, Giannarelli D, Madonna G, Mallardo D, et al. Soluble CD73 as biomarker in patients with metastatic melanoma patients treated with nivolumab. *J Transl Med.* 2017;15(1):244.

46. Theodoraki MN, Hoffmann TK, Jackson EK, and Whiteside TL. Exosomes in HNSCC plasma as surrogate markers of tumour progression and immune competence. *Clinical and Experimental Immunology.* 2018;194(1):67-78.
47. Lee SH, Kim KS, Fodil-Cornu N, Vidal SM, and Biron CA. Activating receptors promote NK cell expansion for maintenance, IL-10 production, and CD8 T cell regulation during viral infection. *J Exp Med.* 2009;206(10):2235-51.
48. Song TL, Nairismagi ML, Laurensia Y, Lim JQ, Tan J, Li ZM, et al. Oncogenic activation of the STAT3 pathway drives PD-L1 expression in natural killer/T-cell lymphoma. *Blood.* 2018;132(11):1146-58.
49. Cacalano NA. Regulation of Natural Killer Cell Function by STAT3. *Front Immunol.* 2016;7:128.
50. Haeussler M, Schonig K, Eckert H, Eschstruth A, Mianne J, Renaud JB, et al. Evaluation of off-target and on-target scoring algorithms and integration into the guide RNA selection tool CRISPOR. *Genome Biology.* 2016;17.
51. Sanjana NE, Shalem O, and Zhang F. Improved vectors and genome-wide libraries for CRISPR screening. *Nature Methods.* 2014;11(8):783-4.
52. Sutlu T, Nystrom S, Gilljam M, Stellan B, Applequist SE, and Alici E. Inhibition of Intracellular Antiviral Defense Mechanisms Augments Lentiviral Transduction of Human Natural Killer Cells: Implications for Gene Therapy. *Human Gene Therapy.* 2012;23(10):1090-100.
53. Sachsenmeier KF, Hay C, Brand E, Clarke L, Rosenthal K, Guillard S, et al. Development of a Novel Ectonucleotidase Assay Suitable for High-Throughput Screening. *Journal of Biomolecular Screening.* 2012;17(7):993-8.

Figure 1

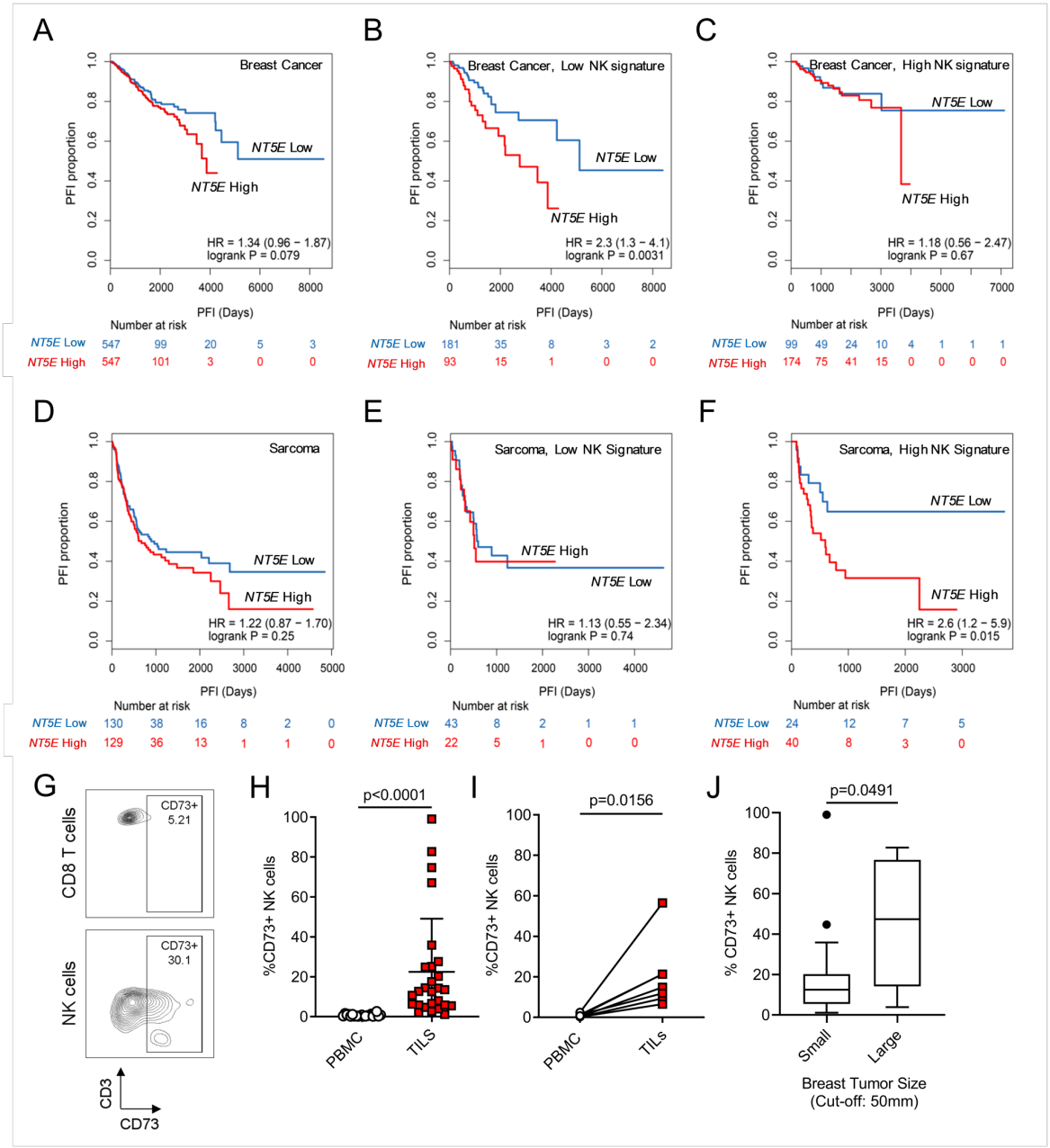

Figure 1.

NT5E expression affects the prognostic value of NK cells in breast cancer and sarcoma patients **A,** *NT5E* expression predicts progression-free interval (PFI) based on TCGA Breast Cancer Cohort (n=1094); **B,** patients with low NK cell gene signature (n=274) and **C,** patients with high NK cell gene signature (n=273). **D,** *NT5E* expression predicts PFI based on TCGA Sarcoma cohort (n=259); **E,** patients with low NK cell gene signature (n=65) and **F,** patients with high NK cell gene signature (n=64). Log rank Mantel-Cox test was used to test for significance. **G,** Representative flow cytometric plot of breast tumor-infiltrating NK cells and CD8 T cells based on CD3 over CD73 expression. (n=25) **H and I**, Differential expression of CD73 by NK cells from peripheral blood versus tumor resections for both breast cancer (n=25) and sarcoma, (n=7) respectively. Mann-Whitney test was used to test for significance in non-autologous comparison in (H) while Wilcoxon signed rank test was used for autologous comparison in (I). **J,** Correlation of percentage CD73+ tumor-infiltrating NK cells with breast cancer tumor size (n=25) based on clinical measurement cut-off (>5cm) Mann Whitney-U rank test was performed to test for significance.

Figure 2

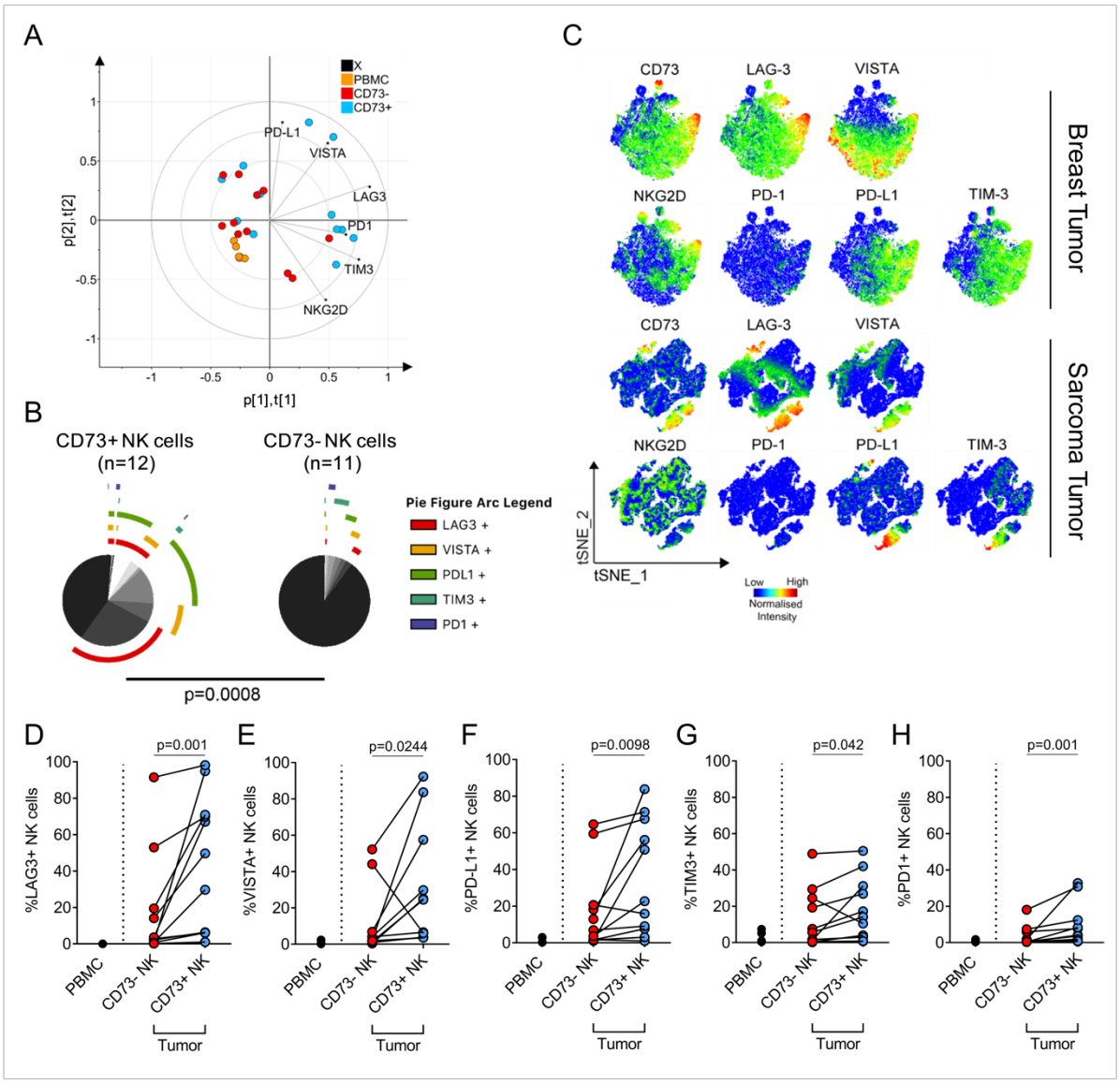

Figure 2.

Characterization of immune checkpoints expression on CD73+ NK cells isolated from 11 individual tumor resections. **A,** Principal component analysis (PCA) analysis showing an overview of heterogeneity in all samples based on their expression of 5 immune checkpoints and NKG2D. **B,** Annotated pie chart showing proportions of cells expressing different combinations of immune checkpoints. Permutation test was performed to compare CD73+ NK cells (n=12) and CD73- NK (n=11) cells. **C,** t-distributed stochastic neighbor embedding analyzed on tumor-infiltrating NK cell populations analyzed from the most representative sarcoma and breast tumor samples. **D to H,** Differential expression of immune checkpoints (LAG-3, VISTA, PD-L1, TIM-3 and PD1) comparing CD73+ NK cells, CD73- NK cells and total peripheral blood NK cells. Paired comparison was done with NK cells analyzed from 7 sarcoma and 4 breast tumor resections. Wilcoxon signed rank test was done to test for significance in matching data points.

Figure 3

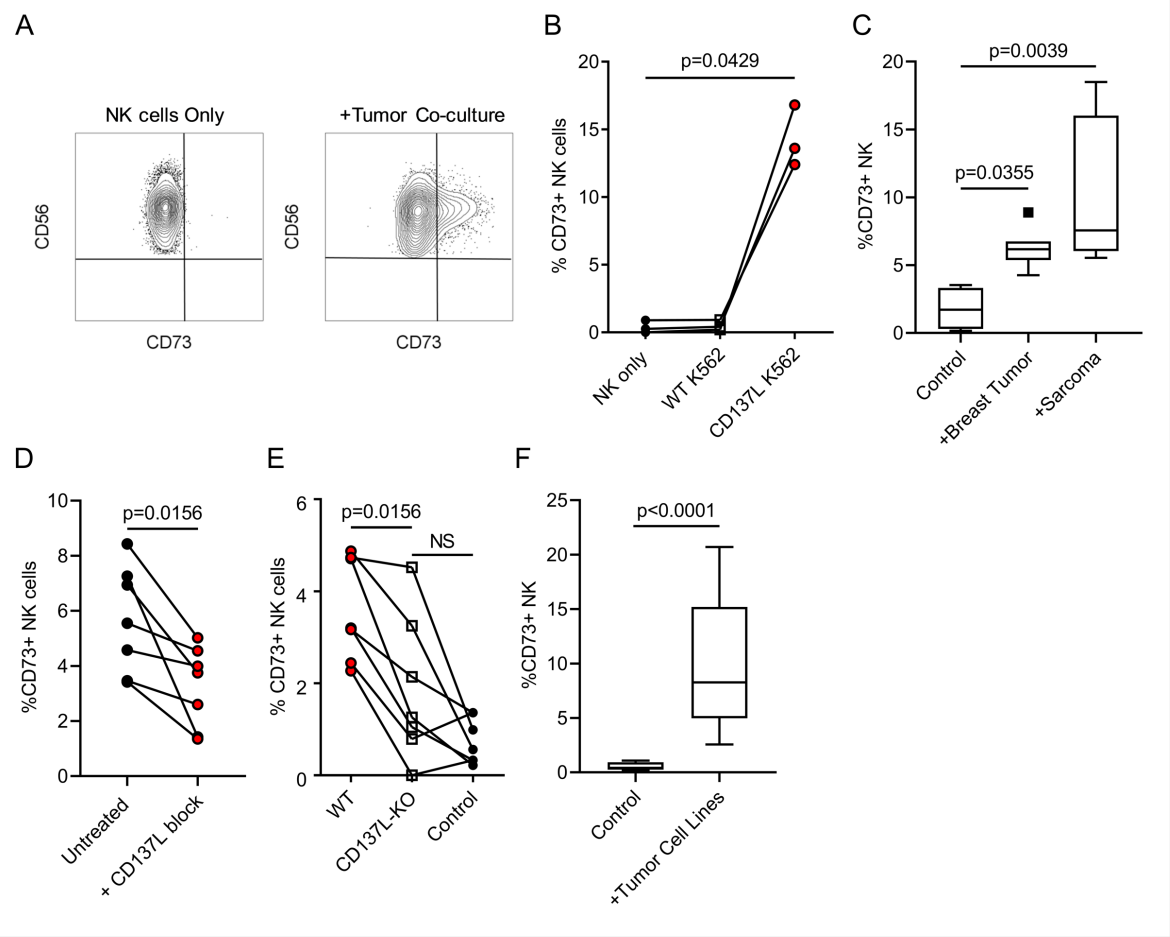

Figure 3.

4-1BBL engagement promotes CD73 surface upregulation on NK cells within 4 hours of tumor co-culture. **A,** Representative flow cytometric plot showing induction of CD73 expression by NK cells after 4 hours tumor co-culture. **B,** Percentage of CD73+ CFSE labelled NK cells after co-culture with fresh patient tumor resections for 4 hours. (n=8 for breast cancer and n=6 for sarcoma) **C,** Percentage of CD73+ NK cells after co-culture with ATCC tumor cell lines (MDA-MB-231, MDA-MB-436, 786O and CAKI2). (n=17) **D,** Percentage of CD73+ NK cells after co-culture with patient-derived sarcoma cell lines in the presence or absence of inhibitory recombinant 4-1BB protein (1µg/ml). (n=6) **E,** Percentage of CD73+ NK cells after co-culture with CD137L knockout patient-derived sarcoma cell lines. (n=7) **F,** Percentage of CD73+ NK cells after co-culture with K562 and K562 transduced with 4-1BBL. (n=3) Friedman test was used to test for significance in matching data points for figures B, D to F.

Figure 4

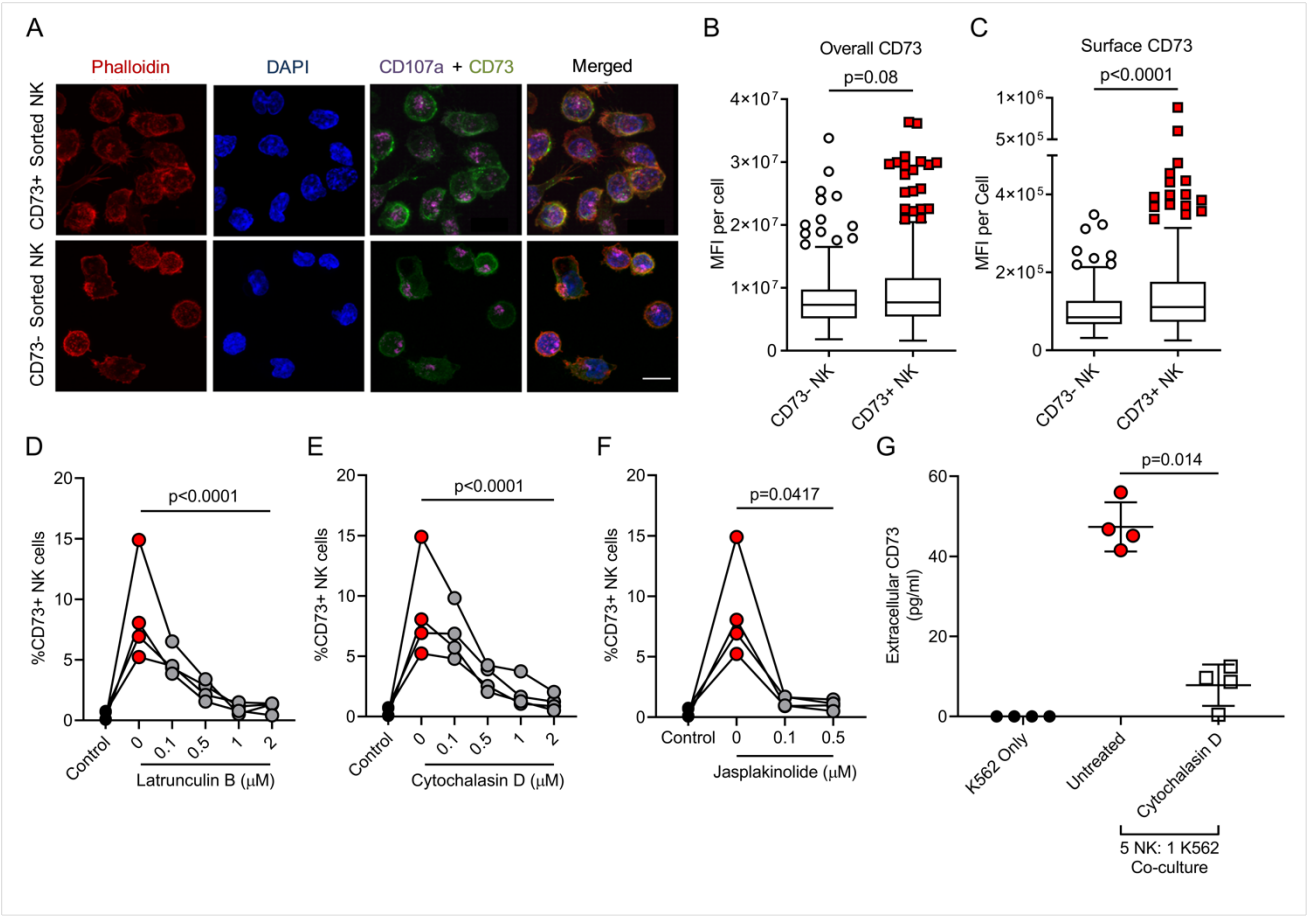

Figure 4.

Tumor cells stimulate NK cells to translocate CD73 into the cell membrane and the extracellular space. **A**, Maximum intensity projection of confocal images showing localization of CD73 and CD107a expression in NK cells sorted after tumor co-culture under 63X objective lens. Scale bar corresponds to 10μm. (n=4) **B,** Overall fluorescence intensity of CD73 staining per cell comparing CD73+ and CD73- NK cells sorted after tumor co-culture. (n=4) **C,** Fluorescence intensity of CD73 on cell membrane of every cell comparing CD73+ and CD73- NK cells sorted after tumor co-culture. (n=4) Significance was tested by Mann Whitney-U rank test for both figure B and C. **D-F,** Dose-dependent inhibition of CD73 surface expression on NK cells after 4 hours co-culture with 4-1BBL transduced K562 in the presence of either Latrunculin B (D), cytochalasin D (E), or Jasplakinolide (F) (n=4) **G,** ELISA assay showing concentration of CD73 protein released after 24 hours of NK cells co-cultured with 4-1BBL transduced K562. (n=4) Friedman test was used to test for significance in figures D to H.

Figure 5

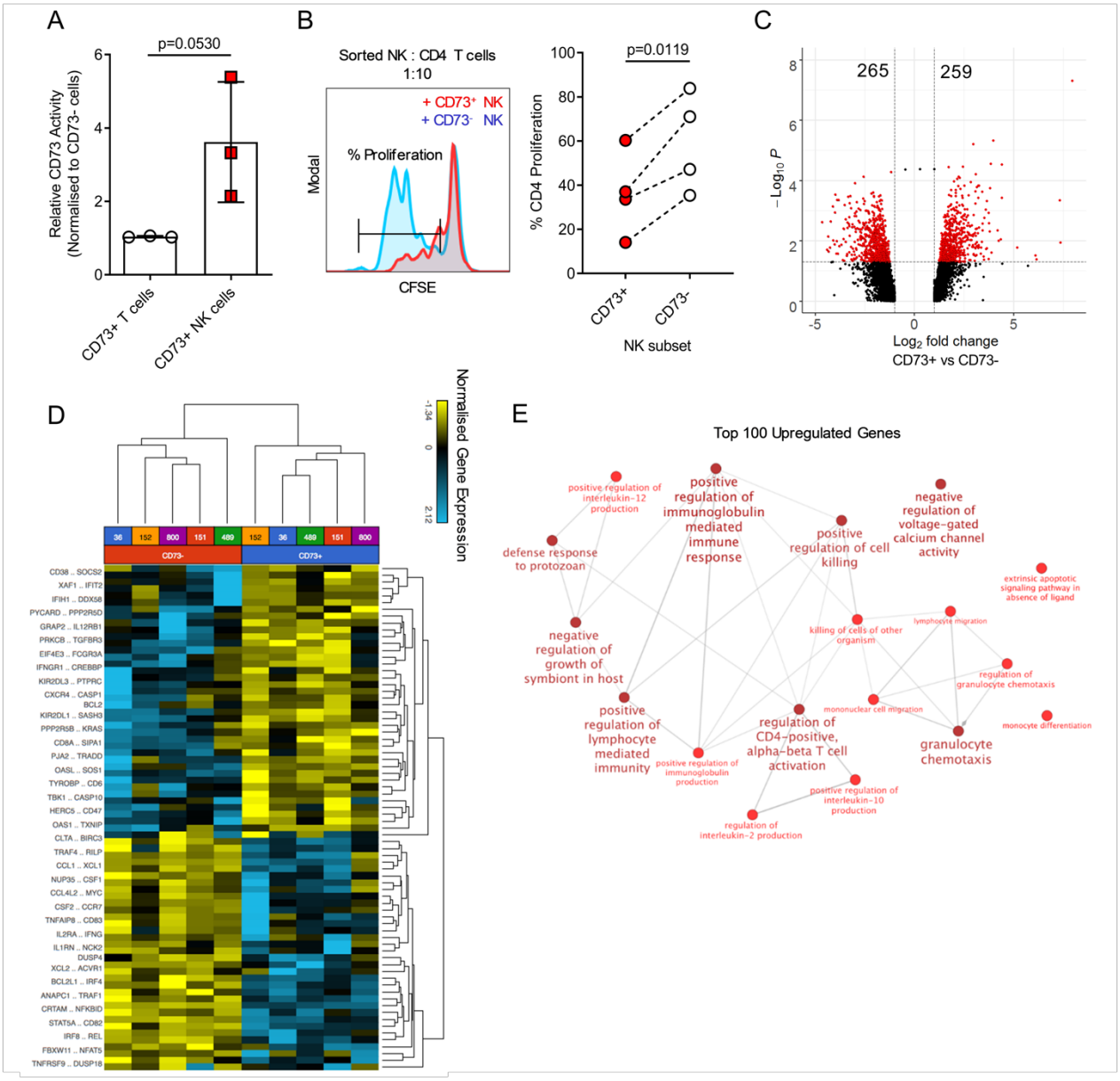

Figure 5.

Characterization of CD73+ NK cells based on differential gene expression. **A,** CD73 enzymatic activity normalized to CD73+ T cells from PBMCs from healthy donors. (n=3) Student t-test was used to test for significance. **B,** Representative histogram and graph showing proliferation of CD4 responder T cells after 2 days of co-culture with different sorted population on NK cells at 10:1 ratio. (n=4) **C,** Percentage of dividing CD4 T cells in 48 hours suppression assay. Significance was tested with Wilcoxon signed rank test. (n=8) **D,** Volcano plot to visualize the significance and magnitude of changes in gene expression comparing CD73+ NK cells versus CD73- NK cells. The X-axis represents the fold change between the two groups and is on log2 scale, and the Y-axis shows the negative log10 of the p-values from mixed-model ANOVA. Genes with significant fold change<2 are represented in red. (n=5) **E,** Gene expression heat map to visualize immune-related genes that are differentially expressed in CD73+ NK cells based on table 4. (n=5) **F,** Gene ontology enrichment analysis visualizing functional pathways for the top 100 genes upregulated by CD73+ NK cells from gene list in table 4. Each node has a minimum of 3 genes and size of the nodes is proportional to the number of genes. Color of the nodes is determined by the significance of the enriched term tested by two-sided hypergeometric test with Bonferroni step down method for p value correction. (n=5)

Figure 6

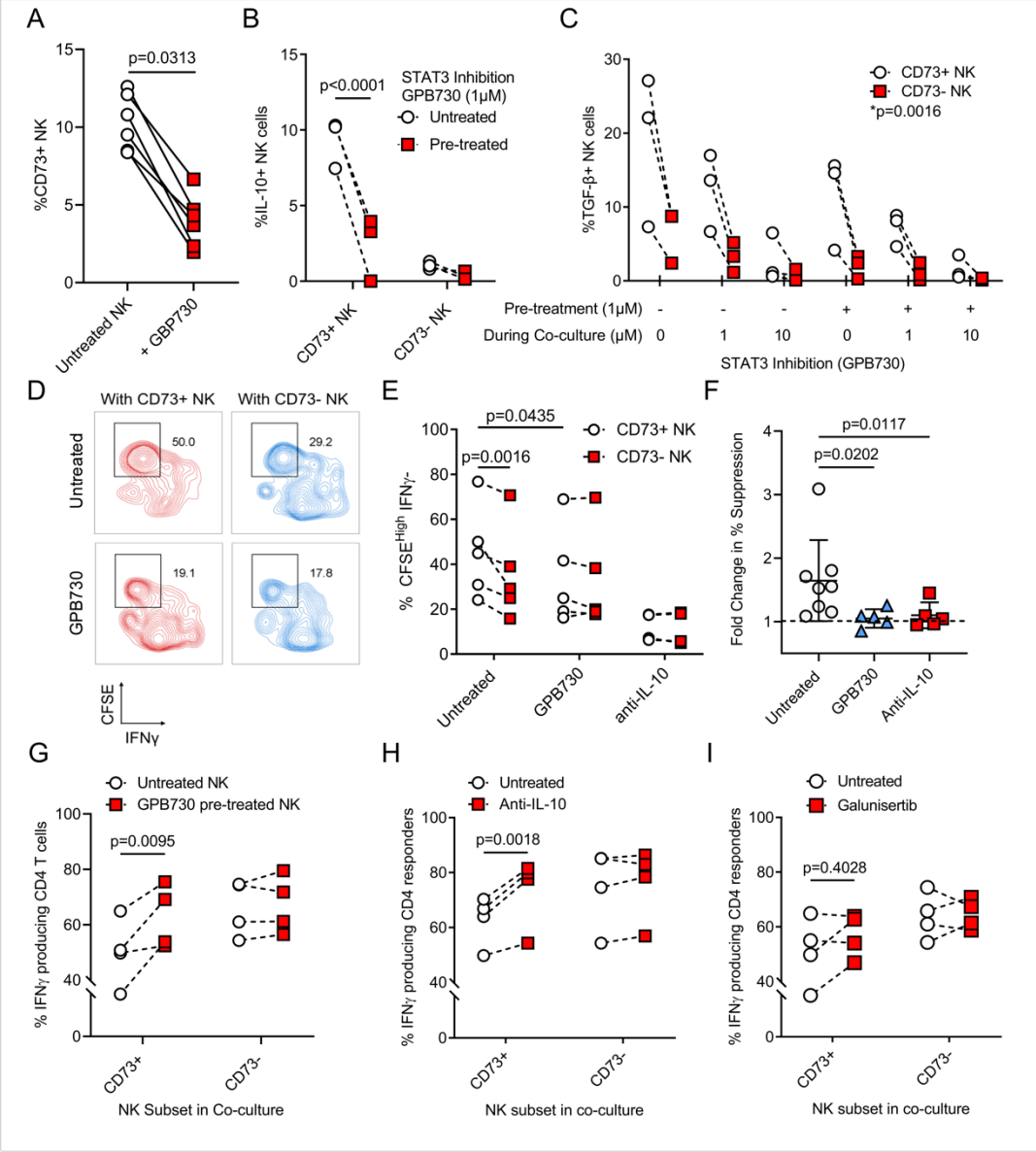

Figure 6.

STAT3-dependent TGF-β and IL-10 production by CD73+ NK cells and suppressed proliferation and cytokine production of CD4 T cells. **A,** Percentage of CD73+ NK cells after treatment with GPB730 (1μM). Wilcoxon signed rank test was done to test for significance. (n=6) **B,** Percentage of IL-10 producing NK cells pre-treated with GPB730 (48 hours at 1μM) prior to overnight tumor co-culture. (n=3) **C,** TGF-β producing NK cells with GPB730 treatment during tumor co-culture. (n=3) *p-value obtained for significant interaction between 2 variables based on two-way ANOVA with Tukey post-hoc test. **D,** Representative set of flow cytometric plot to show percentage of suppressed CD4 based of CFSE and IFN production. (n=5) **E,** Percentage of $CFSE^{high}$ and $IFN\gamma^{negative}$ CD4 T cells after 48 hours of co-culture with different subsets of NK cells at 10:1 ratio. (n=5) Treatment conditions used were NK cells pre-treated with GPB730 (1μM) or co-culture with neutralizing antibody against IL-10 (10μg/ml). **F,** Fold change of percentage suppression (CD73+ vs CD73-) calculated based on percentage of $CFSE^{high}$ and $IFN\gamma^{negative}$ responder CD4 T cells in autologous co-culture. Sample size (n=5) was used in each treated group. Friedman test with multiple comparisons was used to test for significance. **G,** $IFN\gamma^{positive}$ CD4 T cells in a suppression assay comparing sorted CD73+ NK cells versus CD73- NK cells with or without GPB730 pre-treatment. (n=4) **H and I,** $IFN\gamma^{positive}$ CD4 T cells in a suppression assay comparing sorted CD73+ NK cells versus CD73- NK cells in the presence of (I) neutralizing antibody against IL-10 (10μg/ml) and (J) Galunisertib (1μM). (n=4) Repeated measures two-way ANOVA with multiple comparisons were used to test for significant comparisons in figures C, F and H-J.

Table 1: Prognostic Value of CD73 Gene expression Influenced by Immune Gene Signatures in TCGA Sarcoma and Breast Cancer datasets

		NT5E Expression	Sample Size	HR (95% CI) (*NT5E* High vs Low)	p-Value
NK High	Breast Cancer	High	174	1.18 (0.56-2.47)	0.67
		Low	99		
NK Low		High	93	*2.3 (1.3-4.1)	0.0031
		Low	181		
NK High	Sarcoma	High	40	*2.6 (1.2-5.9)	0.015
		Low	24		
NK Low		High	22	1.13 (0.55-2.34)	0.74
		Low	43		
CD8 High	Breast Cancer	High	169	1.12 (0.54-2.32)	0.76
		Low	104		
CD8 Low		High	95	1.53 (0.84-2.78)	0.16
		Low	179		
CD8 High	Sarcoma	High	36	*2.1 (1.1-4.3)	0.03
		Low	28		
CD8 Low		High	22	0.98 (0.49-1.96)	0.95
		Low	43		
FOXP3 High	Breast Cancer	High	181	0.96 (0.45-2.02)	0.9
		Low	92		
FOXP3 Low		High	82	1.57 (0.81-3.06)	0.18
		Low	192		
FOXP3 High	Sarcoma	High	38	1.41 (0.74-2.68)	0.3
		Low	26		
FOXP3 Low		High	33	0.89 (0.45-1.76)	0.74
		Low	32		

*Significant Hazard Ratio

Table 2: Characteristics of Breast Cancer Patient Cohort

	%ER	%PR	%Ki67	Her2 Score	Her2/Neu FISH	NHG^	Tumor size (mm)	Age	Nodes Status
1	100	80	15	1	NEG	2	32	84	POS
2	90	0	14	0	NEG	1	24	70	NEG
3	100	100	24	0	NEG	2	70	68	POS
4	100	90	13	2	NEG	2	30	81	NEG
5	100	70	24	1	NEG	2	17	71	NEG
6	0	0	0	0	NEG	3	18	NA	NEG
7	100	100	24	2	NEG	2	55	NA	POS
8	100	100	23	1	NEG	2	40	NA	NEG
9	95	35	44	0	NEG	2	23	41	POS
10	0	0	81	0	NEG	3	24	45	POS
11	99	93	46	1	NEG	3	40	81	NEG
12	90	70	57	0	NEG	3	31	41	POS
13	99	70	12	1	NEG	1	18	97	NA
14	90	30	28	0	NEG	2	70	67	NEG
15	99	99	51	1	NEG	3	22	71	POS
16	99	90	12	2	NEG	2	30	82	POS
*17**	0	0	98	1	NEG	3	60	43	NEG
18	0	1	96	0	NEG	3	33	83	POS
19	100	35	9	1	NEG	1	14	64	NEG
20	0	0	49	1	NEG	3	16	66	POS
21	0	0	80	0	NEG	3	68	83	POS
22	0	0	81	0	NEG	3	50	90	NA
23	99	0	7	1	NEG	2	37	58	NEG
24	95	60	33	2	NEG	3	17	71	NEG
25	95	99	34	1	NEG	1	5	47	NEG

**Patient receive neoadjuvant treatment*
^NHG: Nottingham Histological Grade
NA: Information not available

Table 3: Characteristics of Sarcoma Patient Cohort

	Subtype	*Tumour*	*Grade*	*Location*	*Genetics*	*Tumour size*
1	Pleomorphic leiomyosarcoma	Primary	Grade 3, (FNCLCC)	Retroperitoneum	Unknown	14 x 14 x 10 cm
2	Myxoid liposarcoma	Primary	Low grade	Subcutaneous, thigh	*FUS-DDIT3* translocation	4,5 x 3,5 x 2,0 cm
3	Metastatic uterine leiomyosarcoma	Metastasis	*n.a.	Intraperitoneal	Unknown	29 x 24 x 12 cm (cystic)
4	Recurrent high-grade chondrosarcoma	Local recurrence	Grade 3, (Evans/WHO)	Peripelvic space	Unknown	11 x 8 x 7 cm
5	Epithelioid hemangio-endothelioma	Primary	High grade	Intraosseous, lower limb	*CAMTA1* translocation	3 x 3 x 2 cm
6	Low grade leiomyosarcoma	Primary	Grade 1, (FNCLCC)	Retroperitoneum	Unknown	8 x 7,5 x 7 cm
7	Metastatic undifferentiated spindle cell sarcoma of the cervix	Metastasis	*n.a.	Intraperitoneal	Unknown	Multiple metastases, the largest 4 cm
8	Chondrosarcoma	Primary	Grade 1 (Evans/WHO)	Proximal Humerus	Unknown	6.1 X 4.1 cm
9	Malignant Peripheral Nerve Sheath Tumor	Primary	Grade 3 (FNCLCC)	Intramuscular, Proximal Leg	*NF1* Mutation	4 X 3 X 2.5 cm

**n.a: Not Applicable*
FNCLCC: French Federation of Comprehensive Cancer Centres
WHO: World Health Organisation